

Facile One-Pot Method of Initiator Fixation for Surface-Initiated Atom Transfer Radical Polymerization on Carbon Hard Spheres

Muhammad Ejaz,¹ Bhanukiran Sunkara,² Lakhinder Kamboj,² Jibao He,³ Vijay T. John,² Noshir S. Pesika,² Scott M. Grayson¹

¹Department of Chemistry, Tulane University, New Orleans, Louisiana 70118, United States

²Department of Chemical and Biomolecular Engineering, Tulane University, New Orleans, Louisiana 70118, United States

³Coordinated Instrument Facility, Tulane University, New Orleans, Louisiana 70118, United States

Correspondence to: S. M. Grayson (E-mail: sgrayson@tulane.edu)

Received 1 February 2013; revised 28 March 2013; published online 22 May 2013

DOI: 10.1002/pola.26728

ABSTRACT: An efficient and novel one-pot process is developed to immobilize the atom transfer radical polymerization (ATRP) initiators onto the surface of fully pyrolyzed carbon hard spheres (CHSs) via a radical trapping process from the *in situ* thermal decomposition of bis(bromomethylbenzoyl)peroxide. The CHSs do not require any additional preparative treatment prior to the initiator immobilization. Styrene and methyl methacrylate are polymerized onto initiator-immobilized CHSs by surface-initiated atomic transfer radical polymerization (SI-ATRP). Samples are characterized using Fourier transform infrared, thermogravimetric analysis, scanning electron microscopy, and transmission electron microscopy.

These methods of characterization confirmed that all the CHSs are coated with a uniform layer of grafted polymer. This efficient, one-pot immobilization of ATRP-initiators represents an exceptionally simple route for the rapid preparation of various polymer-coated carbon-based nanomaterials using SI-ATRP. © 2013 Wiley Periodicals, Inc. *J. Polym. Sci., Part A: Polym. Chem.* **2013**, *51*, 3314–3322

KEYWORDS: atom transfer radical polymerization; carbon hard spheres; nanomaterial; polymer grafts; polystyrene; poly(methyl methacrylate)

INTRODUCTION Carbon hard spheres (CHSs) represent a versatile alternative to traditional metallic or metallic oxide nanoparticles because of their robust character, their unique electronic properties, and their cost-efficient preparation. Well-defined CHSs can be obtained from a wide range of readily available carbon-containing precursors such as methane,¹ glucose,² polystyrene (PSt),³ coal,⁴ kerosene,⁵ and potato starch⁶ using various preparative techniques including arc-discharge processes,⁷ laser ablation,⁸ chemical vapor deposition,⁹ pressure carbonization,¹⁰ and hydrothermal treatment.¹¹ Many of these methods have been optimized to yield particles with fine control over the particle diameter (typically from tens of nms to single μ ms) as well as relatively narrow size distributions.¹² Because of the versatility demonstrated in the preparation of CHSs, they have potential for a broad range of applications, including adsorbents, separation media, catalyst supports, anode material for lithium ion batteries, reinforcement in composite materials, and additives in lubricants.¹² Recent optimization has enabled the rapid synthesis of narrow polydispersed CHSs on a large scale via a hydrothermal carbonization (HTC) process. In addition to providing narrowly disperse CHSs with fine control over the size (between 100 and 2000 nm), the HTC

method is a relatively “green” process, as the many of precursors are biomass-based or are byproducts of petroleum refining and their preparation occurs in pure water at mild temperature without the presences of any hazardous surfactants or catalysts.¹³ Because of their solid nature, spheroidal geometry, thermal stability, chemical purity, and lightweight properties (lighter than graphite and diamond),^{14,15} CHSs show promise as reinforcing agents in light weight composites or “nano-ball bearings” for lubrication applications. However, despite exhibiting attractive mechanical properties, CHSs’ incompatibility with most solvents and bulk polymers results in unstable suspensions, and has prevented their broad utilization. The surface modification of nanoparticles enables their physical properties to be tuned, including wettability, solubility, and dispersibility, and therefore is critical to expanding the applications of CHSs.¹⁶ Although adsorbed surfactants can assist in compatibilizing the CHSs, such surfactants can be readily desorbed, resulting in long-term stability problems leading to aggregation and/or flocculation. The most robust method for improving the dispersibility of CHSs is their covalent functionalization with polymer grafts while the diversity of polymers amenable to grafting offers a broad range of compatibility. With appropriate polymer

grafts, CHSs are expected to yield homogeneous mixtures with a range of polymers, yielding films or bulk materials with enhanced physical and electronic properties. In addition, polymer-grafted CHSs can be optimized for dispersions with a range of liquids, enabling their use as “nano-ball bearing” additives for lubricants.¹⁷ The hardness and chemical robustness of the polymer-grafted CHSs, in addition to their small but uniform size, should yield a high performance lubricant with enhanced resilience at both high temperatures and high pressures.¹⁸

The surface modification of CHSs by covalent attachment of polymer chains to the substrate surface can be achieved via either a “grafting-to” or “grafting-from” approach.^{19,20} The “graft to” approach, generally results in low graft densities due to steric complications.²¹ In the case of the “grafting from” approach, also known as surface-initiated polymerization (SIP), the polymer is grown from initiator attached to the substrate and can yield much more densely packed polymer brushes. Among the SIP methods developed, surface-initiated controlled/“living” radical polymerizations offer both control over the size of the polymer grafts as well as broad compatibility with a range of monomers.^{22–24} Among the different controlled radical polymerization techniques, surface-initiated atom transfer radical polymerization (SI-ATRP) has been used most frequently to produce polymer brushes, because of its chemical versatility: it exhibits compatibility with a variety of monomers and functional groups, it tolerates impurities, and it is relatively insensitive toward residual traces of oxygen. SI-ATRP enables the efficient synthesis of well-controlled polymer brushes with narrow molecular weight distributions on a wide range of surfaces, including: silicon,²⁵ clay,²⁶ gold nanorods,²⁷ magnetite,²⁸ silica,²⁹ polymer films,³⁰ and cellulose.³¹ In addition to preparing well-defined homopolymer grafts, if the ATRP end groups are retained at the terminus of the polymer grafts, they can be reinitiated to yield block copolymer grafts.³² These combined advantages of SI-ATRP enable the surfaces of particles to be readily tailored to exhibit the desired physicochemical properties for a wide range of applications.³³ Although SI-ATRP has already been used in an effective way for the surface modification of nanostructured carbon materials such as carbon black nanoparticles, carbon nanotubes, CHSs, and graphene/graphene oxide,^{34–38} these involved a multistep preparation of the surface. For example, recently Gao and co-workers³⁹ functionalized the pure CHSs surface with ATRP initiator in four steps to produce polymer grafted CHSs by SI-ATRP. First, the pristine CHSs were oxidized with concentrated nitric acid, producing surface carboxylic acid groups, which were then reacted with SOCl_2 in the second step to produce acid chloride functionalities, in the third step those functionalities were treated with an excess of ethylene glycol to yield surface hydroxyl groups and finally in the fourth step the initiator functionalized CHSs were prepared by esterification of the alcohol groups with 2-bromo-2-methyl propanoyl bromide. The harsh acidic conditions used may lead to degradation of the CHS core, while the low efficiency of multistep solid phase reactions results in lower densities

of surface reactive sites. Unlike previous conventional immobilization techniques of initiator, our radical-based strategy does not involve any harsh oxidizing acidic conditions and can be achieved in a single step via radical fixation.

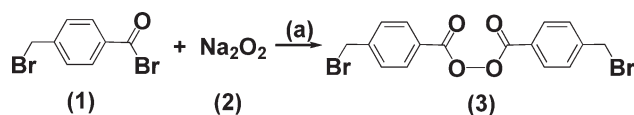
A radical fixation route is an ideally suited method for surface immobilization onto CHSs. The CHSs have many open-ended graphitic flakes and an abundance of defects on the surface, which give them high surface chemical activity.⁴⁰ It is well known fact that carbon materials like carbon black are strong radical scavengers.⁴¹ Tsubokawa and co-workers^{42,43} reported that radical polymerizations in the presence of carbon black were inhibited and/or retarded, because of the surface trapping of primary radicals and growing polymer radicals by carbon black. Although part of the polymer could be grafted onto the surface, a very low percentage of polymer mass could be grafted, because of preferential trapping of low molecular weight primary radicals formed by the decomposition of initiator. However, this radical trapping behavior can also be used to efficiently functionalize the surface of graphitic materials. For example, Ying et al.⁴⁴ reported the derivatization of small-diameter single walled carbon nanotubes via free radicals generated by the decomposition of benzoyl peroxide in the presence of alkyl iodide. Terrones and coworkers⁴⁵ also recently reported the two-step fixation of ATRP initiators on single-walled carbon nanotubes. Therefore, we have explored taking advantage of the radical-trapping ability of the CHS surface to immobilize the initiator groups, while quenching much of this activity to minimize the inhibiting effect during subsequent SI-ATRP.

Herein, we describe CHSs with well-defined polymer grafts by carrying out SI-ATRP from pristine CHSs in only two synthetic steps. In this work, CHSs were produced by the hydrothermal process from aqueous sucrose solution. We developed a one-step method for covalent immobilization of an ATRP initiator with benzyl bromide moieties on the fully pyrolyzed CHSs without any prior functionalization. The initiator-coupled CHSs could be used directly to prepare graft polymer chains via SI-TARP, including PSt and poly(methyl methacrylate). This work represents one of the most efficient methods yet reported for the grafting of ATRP initiators from carbonaceous materials. Our strategy of fixation of initiator has three major advantages: it avoids acid treatment, it involves only one step for initiator immobilization and it minimizes the inhibiting/retarding effect of CHSs in SI-ATRP. The synthetic efficiency of this route should broaden the commercial viability of polymer grafted nanoparticles for a variety of materials applications.

EXPERIMENTAL

Materials

Styrene (99%, Sigma-Aldrich) was purified by passing through neutral alumina. Methyl methacrylate (99%, MMA) was purified by passing through basic alumina. Copper (I) bromide (98%, Sigma-Aldrich) was purified by stirring over boiling glacial acid (Fisher Scientific) then washing the solid



SCHEME 1 Synthetic scheme of *bis*-(bromomethylbenzoyl)peroxide BBMBPO. Reagents and conditions: (a) Diethylether/water, 0 °C to room temperature, 2 h.

residue with ethanol and diethyl ether, and finally drying overnight under vacuum. *N,N,N',N'',N'''*-pentamethyldiethylenetriamine (PMDETA, 99%, Sigma-Aldrich) 4,4'-dinonyl-2,2'-dipyridal (DNNDP, 97%, Sigma-Aldrich), 4-methylbenzyl bromide (MBB, 97%, Aldrich), sodium peroxide (97%, Sigma-Aldrich), 4-bromomethylbenzoyl bromide (BMBB, 96%, Sigma-Aldrich), sucrose (ACS reagent Sigma-Aldrich), and all other reagents were used as obtained from commercial sources without additional purification. The CHSs were produced by the hydrothermal process,¹¹ whereby 0.5 M aqueous solution of sucrose was hydrothermally treated in pressure cylinders at 190 °C for 6 h. The resultant suspension was centrifuged, washed repeatedly with water and ethanol and oven dried at 50 °C. The samples were then carbonized at 1000 °C in a tube furnace under N₂ atmosphere for up to 24 h.

Synthesis of Bis(bromomethylbenzoyl)peroxide

The initiator precursor *bis*-(bromomethylbenzoyl)peroxide (BBMBPO) was synthesized as follows (Scheme 1)^{46,47}: 5.00 g (17.98 mmol) of BMBB in 40 mL of diethyl ether was added dropwise to 8.24% aqueous solution of 1.4 g (17.98 mmol) of sodium peroxide while stirring at 0 °C. Upon completion of the addition of BMBB, the reaction mixture allowed to warm to room temperature and stir for an additional 2 h. The white precipitate was filtered, washed with water and diethyl ether and dried under vacuum for about 2 h. The crude product was recrystallized from chloroform to form white solid in 51% yield.

¹H NMR (CDCl₃, δ, ppm) 4.5 (s, 4H, CH₂Br), 7.5 (s, 8H, ArH), 8.0 (8H, ArH).

Immobilization of ATRP Initiator onto CHSs by Radical Coupling

10 milligram of CHSs were dispersed in 50 mL of toluene and sonicated for 20 min. 0.75 g (1.75 mmol) of BBMBPO was then added to above mixture. After purging with Ar for 30 min, the reaction was initiated by heating to 105 °C and stirred vigorously under Ar for 6 h. Afterwards, the modified CHSs were collected by repeated dispersal into solvent by sonication, and then centrifugation. The solvent series used was first toluene, then dichloromethane, then tetrahydrofuran (THF), and then methanol. The cleaned CHSs were then dried under vacuum overnight.

Surface-Initiated Atomic Transfer Radical Polymerization of Styrene

The initiator functionalized CHSs were used to initiate the ATRP, and a representative example (with styrene monomer) is provided below. 10.00 mg of initiator-functionalized CHSs were dispersed in mixture of 5 g (48.01 mmol) of styrene

and 5 g of anisole in a 25 mL Schlenk flask equipped with a stir bar. After a 30 min Ar purge, 72 mg (0.50 mmol) of CuBr was added to above suspension under an Ar flow followed by addition of 119 mg (0.68 mmol) of PMDETA and 17.00 mg (0.096 mmol) of MBB as free initiator. The ratio of the initial monomer concentration ([M]₀) and initiator concentration ([I]₀) ratio was 500. The flask was placed in a thermostatic oil bath at 95 °C and the suspension was stirred for 29 h in an Ar atmosphere. The product was then diluted with THF. The PSt-grafted CHS particles were isolated from free PSt by repeated dispersal in THF by bath sonication, centrifugation, and decanting the free PSt solution. Trace amounts of CuBr were removed by additional washes of MeOH/THF, aqueous NH₄Cl/THF and H₂O/THF solvents. Finally, the CHSs-PS particles were vacuum dried overnight. The SI-ATRP of styrene on CHSs was also carried out in absence of the free initiator by following the procedure described above but omitting the addition of MBB. The [M]₀/[I]₀ was 18,000.

Surface-Initiated Atomic Transfer Radical Polymerization of MMA

15.00 mg of ATRP initiator functionalized CHSs were dispersed in mixture of 7.5 g (75.0 mmol) of MMA monomer and 7.5 g of anisole in 25 mL Schlenk flask equipped with a stir bar and purged with Ar for 30 min. 21.4 mg (0.15 mmol) of CuBr was added to above mixture under an Ar flow followed by addition of 122.2 mg (0.30 mmol) of DNNDP and 27.7 mg (0.15 mmol) of MBB as free initiator. The [M]₀/[I]₀ was 490. The flask was placed in a thermostated oil bath at 95 °C and the mixture was stirred for 2 h under an Ar. The mixture was then diluted with THF. The CHS-PMMA particles were isolated from free PMMA by repeated dispersal in THF by bath sonication and centrifugation as described above. The trace amounts of CuBr were removed with solvent washes as described above. The CHSs-PMMA particles were finally vacuum dried overnight. The SI-ATRP of MMA on CHSs was also done in absence of the free initiator as described above but without addition of MBB. The [M]₀/[I]₀ was 19,000.

Instrumentation

¹H NMR (400 MHz) spectrum was obtained on a Varian Mercury spectrometer (Palo Alto, CA) using the TMS peak for calibration. Size exclusion chromatography was carried out on Waters model 1500 series pump (Milford, MA) with three-column series from Polymer Laboratories, consisting of PLgel 5 μm Mixed C (300 × 7.5 mm²) and PLgel 5 μm 500 Å (300 × 7.5 mm²) columns. The system was fitted with a Model 2487 differential refractometer detector. THF was used as mobile phase (1 mL/min flow rate). The calculated molecular weight was based on calibration using linear PSt standards. Data was collected and processed using Precision Acquire software. The Fourier transform infrared (FTIR) spectroscopy was performed using a NEXUS 670 FT-IR SEP. Analyte was mixed with KBr and ground into a fine powder by mortar and pestle and compacted into a pellet by applying pressure. Thermogravimetric analysis (TGA) data was acquired using TA Instruments TGA 2950 Thermogravimetric Analyzer with heating rate of 10 °C per minute under N₂

atmosphere. Data was processed using TA Instruments Universal Analysis software. Transmission electron (TEM) microscopy data was collected with a JEOL 2010 operated at 200 kV. Field emission scanning electron microscopy (SEM) data was obtained using Hitachi S-4800, operated at 20 kV. The SEM samples were prepared by putting the fine solid powder of particles onto carbon conducting tape.

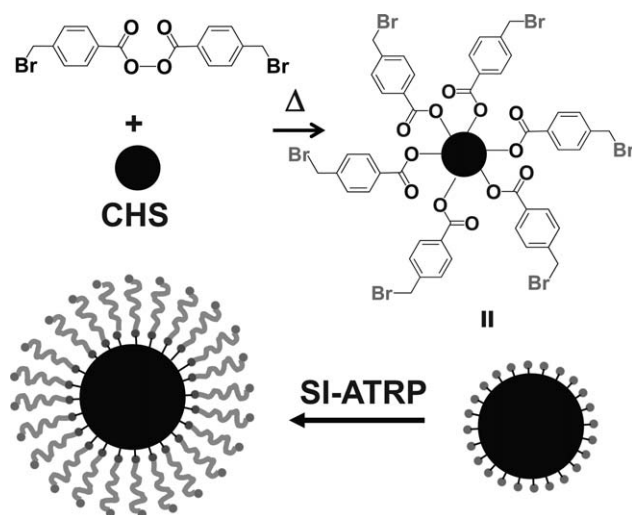
RESULTS AND DISCUSSION

Synthesis of CHSs

Spherical, porous CHSs were prepared by a hydrothermal method.¹¹ The measured Brunauer–Emmett–Teller surface area was around 320 m²/g and average pore size measured from the high resolution TEM (HRTEM) image was of about 0.4–1.5 nm.

Immobilization of Bis(bromomethylbenzoyl) Peroxide (BBMBPO) on CHSs

To carry out SI-ATRP on CHSs, the ATRP initiator must first be immobilized on surface of CHSs. Generally the ATRP initiators are immobilized on carbon materials in multiple steps. In this work, we explored free radical addition of BBMBPO^{40,47} as a 1 step initiator fixation process to the CHS surface (Scheme 2). It has been reported that graphitic surfaces have a reproducible free radical acceptor ability.⁴⁸ At 105 °C, BBMBPO decomposes into free radicals that can form covalent bonds directly with the conjugated graphitic surface, as well as defect sites. Similar reactivity has been noted for the radical surface grafting of multi-walled nanotubes.^{44,45,49} As a result of this reaction, benzyl bromide functionalities are covalently attached onto the surfaces of CHSs that can act as initiators for SI-ATRP of styrene and MMA⁵⁰ (Scheme 2). Unreacted initiator was washed from the particles by repeated suspension, centrifugation, and decanting of the supernatant. The dispersibility of particles after treating with coupling agent was improved significantly in organic solvents such as toluene or anisole. This method represents a simple,



SCHEME 2 Stepwise SI-ATRP process for grafting polymer brushes from CHSs.

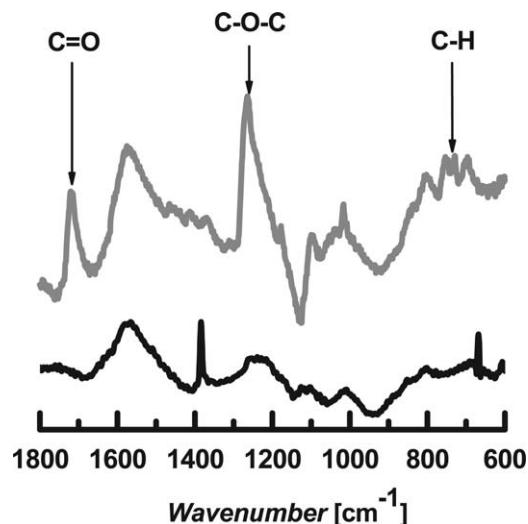


FIGURE 1 FTIR spectra of (below) pristine CHSs and, (above) CHSs-BBMBPO.

rapid route for the surface attachment of ATRP initiators and is particularly useful for large-scale syntheses.

The surface attachment of initiator could be confirmed by infrared spectroscopy and TGA. In the FTIR spectra of CHSs, there are few characteristic signals, as expected for a fully pyrolyzed graphitic surface [Fig. 1(a)]. However after the reaction with BBMBPO, the spectrum [Fig. 1(b)] of modified CHSs exhibits characteristic peaks, including a carbonyl band located at 1730 cm⁻¹ and an ester C–O band at 1270 cm⁻¹. Finally, the presence of aromatic rings is suggested by the very weak signal located at 735 cm⁻¹, representing the resonance of aryl hydrogen atoms.

The grafting of the initiator could be further confirmed by the addition of pyrolyzable weight onto the CHSs during TGA studies. The thermograms of the pristine CHSs and initiator immobilized CHSs are shown in Figure 2. The pristine CHSs

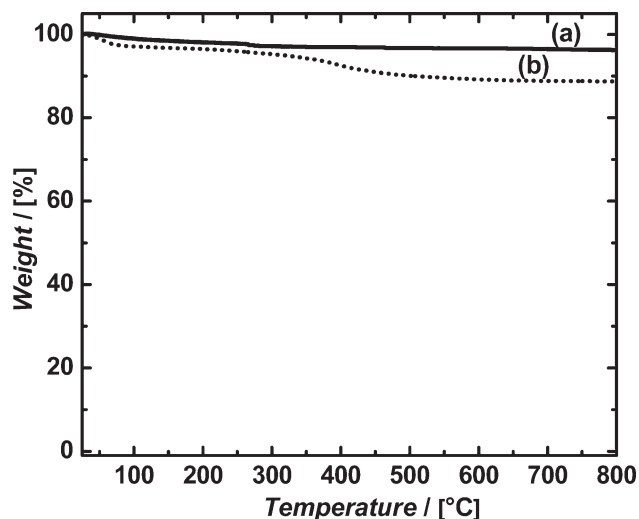


FIGURE 2 TGA curves of (a) pristine CHSs, (b) CHSs-Br.

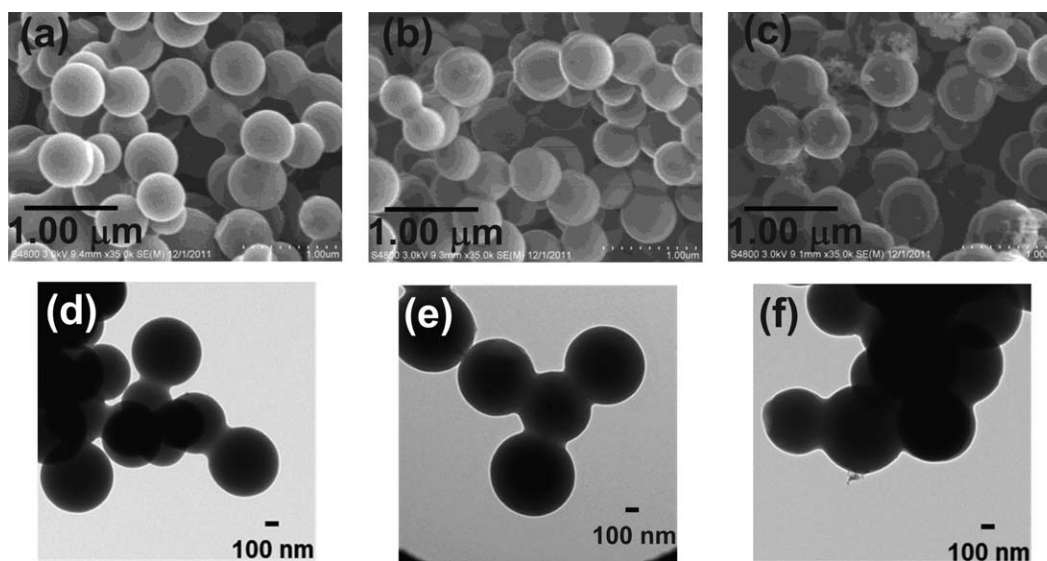


FIGURE 3 SEM images of (a) Pristine CHSs, (b) CHSs-BMBPO and (c) CHSs-PSt-FI. TEM images of (d) Pristine CHSs (e) CHSs-BMBPO, and (f) CHSs-PSt-FI.

exhibit a good stability at high temperatures, with only 2% weight loss at 800 °C in an inert atmosphere. However, BBMBPO-immobilized CHSs (CHSs-Br) exhibit a measurable loss of mass between 300 and 500 °C with 157 °C onset temperature point and 405 °C inflection temperature point that represents about 5% of the sample's total weight. The initiator concentration and density calculated from this 5% weight loss difference from the modified CHSs to pristine CHSs indicate approximately 2.8 initiator moieties per 1000 carbons or 0.233 mmol per g. This concentration is very near to those reported in similar studies of CHSs (3.4 initiators per 1000 carbons, or 0.268 mmol per g) that required multiple steps for initiator fixation.³⁹ The porous CHSs used in this study have surface area 320 m²/g and average pore sizes of about 0.4–1.5 nm (measured from image of the HRTEM microscope). From the above data the calculated surface initiator density is about 0.47/nm², which includes the surface of the nanopores within the overall surface area measurements. FTIR analysis provides further evidence of surface grafting, as the change in IR spectra upon reaction with BBMBPO corresponds to a combination of grafted side wall aromatic rings, and the distorted fragments of the external CHSs layers. In addition, the increased tendency of the modified CHSs to form suspensions in organic solvents such as toluene, anisole, chloroform and THF further demonstrates that the CHSs' surface has been modified to a substantial extent with organic moieties.

The field emission SEM and TEM studies, on the other hand, show little change in the size or morphology upon surface modification. As prepared, the CHSs appear as aggregates that could be clearly visualized in both the SEM [Fig. 3(a)] and TEM [Fig. 3(d)]. Upon initiator fixation, there was no obvious change in structure observed in either the SEM [Fig. 3(b)] or the TEM [Fig. 3(e)]. These results are expected, as the sub-nanometer thickness of the initiating groups are

negligible compared to the ~500-nm diameter nanoparticles. These data confirm that the surface immobilization of the ATRP initiator can be achieved with a substantial amount of surface functionalities, but without substantially altering the morphology or integrity of the CHSs substrate.

SI-ATRP of Styrene and MMA from Initiator-Immobilized CHSs

The SI-ATRP was tested via the polymerization of two common monomers, namely, styrene (St), and MMA. Both were polymerized in anisole solvent at 95 °C from the initiator-functionalized CHSs using the CuBr/PMDETA catalytic system for 29 h or the CuBr/ DNDP catalytic system for 2 h for St and MMA, respectively. In both cases the polymerizations were carried out twice, once in the presence of an analogous, unimmobilized free initiator, MBB and once without it (but otherwise identical polymerization conditions). The sacrificial initiators are typically used in SI-ATRP to control the polymerization. The generated soluble polymer can also be used as an indirect measurement of molecular weight and polydispersity index of the surface grafted polymer chains, assuming that the kinetics of surface polymerization is similar to that in solution by fast exchange process.^{51–53} The free polymer formed in the solution was separated from the grafted CHSs by centrifugation, and characterized by GPC. A molecular weight of 81,000 with a PDI around 1.43 was observed by GPC for the free PSt produced in the SI-ATRP experiment in the presence of the sacrificial initiator (~80% conversion of monomer) while molecular weight of 144,000 with a PDI around 1.60 was detected by GPC for free PSt produced in SI-ATRP experiment without any sacrificial initiator (~20% conversion of monomer). The latter soluble polymer was formed by adventitious solution phase initiation. There is strong possibility of thermal initiation of monomer in solution. For the PMMA polymerizations, a molecular weight of 46,000 with a PDI around 1.37 was observed for free PMMA

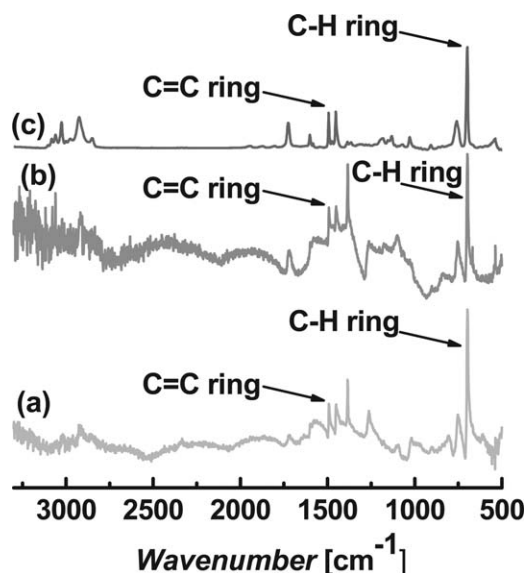


FIGURE 4 FTIR spectra of (a) CHSs-PSt-NFI, (b) CHSs-PSt-FI, and (c) PSt.

produced from sacrificial initiator (~60% conversion of monomer) while a molecular weight of 171,000 with a PDI around 1.57 was detected by GPC for free PMMA produced in the absence of sacrificial initiator (~15% conversion of monomer). The latter soluble polymer was formed by adventitious solution phase initiation, though the source of initiation is unclear. The reduced polydispersity and polymer molecular weights observed with sacrificial initiator implies that for both monomers the polymerization is more controlled by the addition of sacrificial initiator than without it. It should be noted here that when there was low concentration of overall initiators (both immobilized and free), and higher ratios of monomer to initiator, there was little amount of deactivating Cu^{II}/Br₂ species generated, which resulted in polymer with higher molecular weight and broad PDI.

When the concentration of overall initiator was increased by adding free sacrificial initiator, there is more control over polymerization and molecular weight control during ATRP can be achieved via the persistent radical effect.⁵⁴ From “free initiator” to “no free initiator” polymerization there is significant increase in molecular weight of free polymer. The polymer grafted particles demonstrated improved colloidal stability in organic solvents (good solvents for polymer corona) than bare particles which exhibited negligible compatibility in all solvents.

The bromobenzyl initiator was selected because of its efficient mode of attachment onto the CHSs, however, a more efficient initiator will likely yield improved graft densities, increased molecular weights, and reduced polydispersities.

The polymer grafted CHSs were characterized qualitatively by FTIR spectroscopic studies to verify the presence of surface-bound polymer. Characteristic PSt signals were observed in the FTIR spectra of PSt without added free initiator [CHSs-

PSt-NFI, Fig. 4(a)] and with added free initiator [CHSs-PSt-FI, Fig. 4(b)] including the aromatic C=C ring stretches (1453 and 1493 cm⁻¹). For PMMA-grafted CHSs without [Fig. 5(a)] and with [Fig. 5(b)] free initiator, strong ester carbonyl signals were observed at 1730 cm⁻¹. The presence of dense polymer grafts on the CHS surfaces could be further confirmed by their substantially improved dispersibility in good solvents for the corresponding polymer grafts, such as THF or CHCl₃.

A control experiment was carried out in which pristine CHSs, without immobilized ATRP initiator, were subjected to identical polymerization conditions as the above graft polymerization from CHSs. FTIR studies suggest that no grafted polymers were formed. The spectra of pristine particles were almost identical before and after these control experiments.

To quantify the amount of grafted polymer relative to the CHS core, TGA was used to characterize the CHSs-polymer grafted samples. All of initiator moieties and polymers are assumed to be completely pyrolyzed at 800 °C leaving only the residual CHS cores. Figure 6(a,b) indicate that the grafted PSt decomposes around 500 °C with 310 °C onset temperature point and 480 °C inflection temperature point from both of the PSt grafted CHSs which is comparable to the decomposition of pure PSt with an onset temperature of 387 °C and an inflection temperature point at 465 °C [Fig. 6(c)]. After 29 h of polymerization in the presence of free initiator, it can be concluded that PSt was grown from CHSs-PSt-FI, representing about 9.1% of the particles overall mass [Fig. 6(a)]. For the PSt-grafted CHSs prepared in the absence of free initiator, an increased mass of grafting (17.47% PSt by mass) was grown from CHSs-PSt-NFI, [Fig. 6(b)] during the same time of polymerization. The above results show that the amount of grafted PSt on CHSs can be controlled simply by tuning the amount of sacrificial initiator added without changing other parameters. Furthermore, Figure 7(a,b)

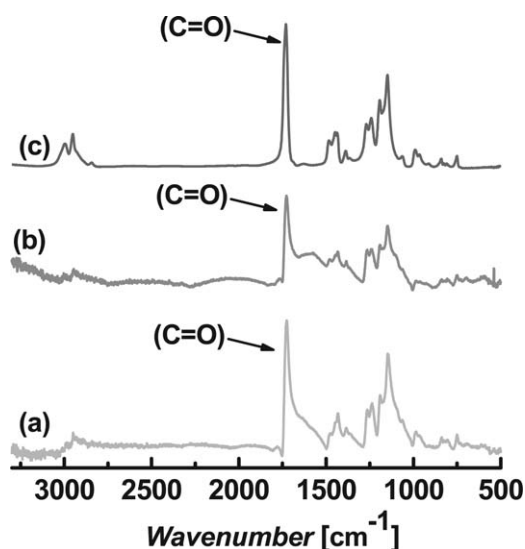


FIGURE 5 FTIR spectra of (a) CHSs-PMMA-NFI, (b) CHSs-PMMA-FI and (c) PMMA.

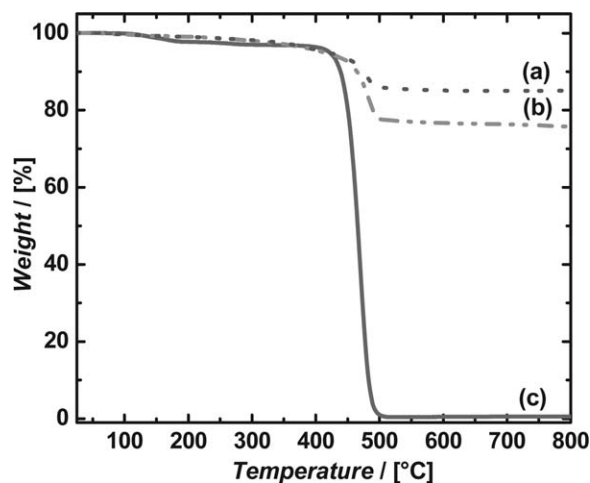


FIGURE 6 TGA curves of (a) CHSs-PSt-FI (b) CHSs-PSt-NFI, and (c) PSt.

indicates that the grafted PMMA decomposes with an onset temperature of about 256 °C and an inflection point at 445 °C which is comparable to decomposition of pure PMMA [Fig. 6(c)] with an onset temperature of 312 °C and an inflection temperature point at 420 °C. After 2 h of polymerization in the presence of free initiator, CHSs-PMMA-FI, [Fig. 7(a)] consisted of 16.3% by mass of PMMA whereas for CHSs-PMMA-NFI, prepared in the absence of free initiator, 35.4% of the overall mass corresponded to PMMA, [Fig. 7(b)]. The increase in weight loss from “free initiator” to “no free initiator” samples is simply due to the increase in molecular weight of the polymer brushes on the surface during polymerization. Like PSt system above results show that the molecular weight of grafted PMMA chains on CHSs can be controlled simply by changing the feed ratio of monomer to overall initiators (free and surface-bound).

Based on the TGA analyses, surface area of CHSs, the reported density of polymer in bulk and the presumed molecular weight of grafted polymer, (based on soluble polymer

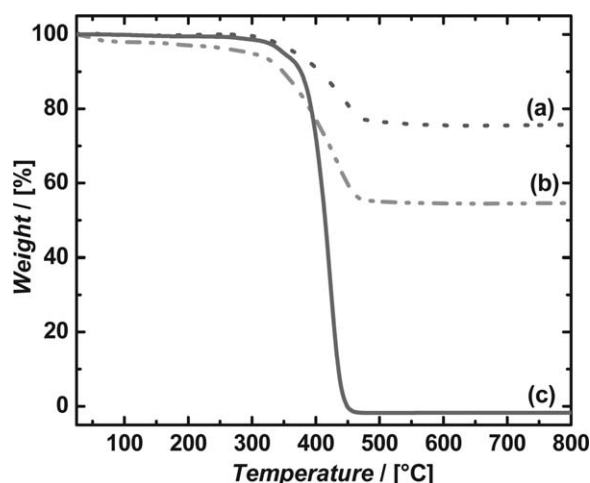


FIGURE 7 TGA curves of (a) CHSs-PMMA-FI (b) CHSs-PMMA-NFI, (c) PMMA.

fraction) the polymer graft densities on the CHSs can be calculated. The computed values are 0.0021 and 0.0023 chains/nm² for CHSs-PSt produced in the presence of free sacrificial initiator and without it respectively. Similarly graft densities of PMMA were calculated: 0.0068 and 0.0039 chains nm⁻² with and without sacrificial initiator, respectively. One possible reason for this low density of polymer brushes relative to PSt brushes on silicon wafers (about 0.40 chains nm⁻²)⁵⁵ and PMMA brushes on gold nanoparticles (about 0.30 chains nm⁻²)⁵¹ might be the presence of nanometer sized pores on the surface of CHSs resulting in narrow inner pore's surface areas that are incapable of grafting large polymer chains. It should be clarified that the above graft density calculations include the surface area of any pores or cavities that may be present on the outer surface. Because the values of graft densities for both PSt and PMMA systems have same order of magnitude, it is believed that the technique is highly reproducible, and the incorporation of unbound, “free initiator” has little effect on the overall graft densities.

SEM and TEM studies enable us to investigate the nanoscale morphologies and the surface structure of polymer grafted CHSs. Figure 3(b,c) present typical SEM images of CHSs initiator immobilized and CHSS-PSt-FI, respectively. In both images, CHSs are with almost same overall shape as pristine CHSs. In TEM observations, the polymer phase is brighter than the CHSs phase because more electrons are transmitted through the polymer regions than through the CHS regions. A typical TEM image of polymer-grafted CHSs is shown in Figure 8(b). The CHSs are completely enveloped by a visible continuous and uniform smooth film of grafted PSt as compared to initiator-grafted CHSs [Fig. 8(a)]. Similarly results were observed in TEM studies of CHSs-PMMA revealing a continuous and uniform smooth film of grafted PMMA. In HRTEM images, the polymer grafts can be more easily distinguished from the CHS core [Fig. 9]. In case of the fusion points of pristine particles, the high and lower contrast diffused continuously without any definite sharp boundary between them whereas in the case of polymer grafted particles, there is very clear sharp boundary (interface) between lower contrast (polymer layer) and carbon particles. From these images the thickness of the PSt grafted films are calculated to be 19.4 and 32 nm in case of CHSs-PSt produced in the presence [Fig. 9(a)] and absence of sacrificial initiator

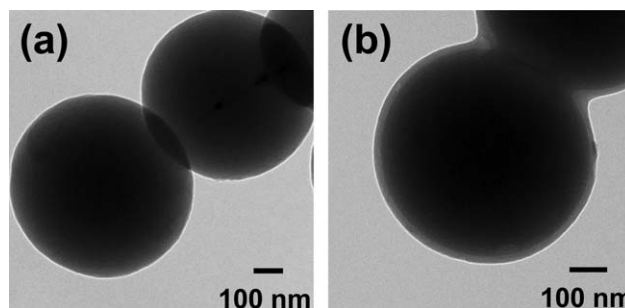


FIGURE 8 TEM images of (a) CHSs-BBMBPO, and (b) CHSs-PSt-FI.

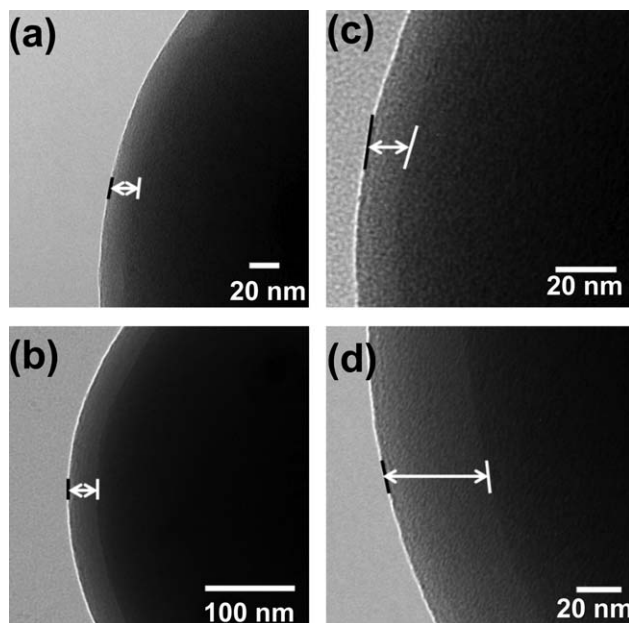


FIGURE 9 HRTEM images of (a) CHSSs-PSt-FI, (b) CHSSs-PSt-NFI (c) CHSSs-PMMA-FI, and (d) CHSSs-PMMA-NFI.

[Fig. 9(b)], respectively. For the PMMA grafted CHSSs, HRTEM revealed thicknesses of 13.0 and 47.0 nm in case of CHSSs-PMMA produced in the presence of [Fig. 9(c)] and absence of sacrificial initiator [Fig. 9(d)], respectively. Based on the film thickness values obtained from HRTEM images, the bulk density of polymers and molecular weight of grafted polymer, which was assumed equal to the corresponding free polymers, the graft densities (σ) of polymer grafted chains on CHSSs can be calculated by an alternative formula:

$$\sigma = (h\rho N_A) / M_n \quad (1)$$

where h is polymer film thickness; ρ is bulk density of polymer; M_n , molecular weight of polymer and N_A , Avogadro's Number.

The calculated values are 0.143 and 0.137 chains/nm² from CHSSs-PSt produced in the presence of free sacrificial initiator and without it, respectively. Similarly densities of PMMA grafted chains are 0.173 and 0.172 chains/nm² from CHSSs-PMMA produced in the presence of free sacrificial initiator and without it, respectively. These values are much closer to the commonly reported graft densities of polymer brushes by SI-ATRP from nanoparticles⁵¹ because in these calculation the effective external surface area, rather than the whole porous surface area is used in the calculation. From these values, it is revealed that high density polymer brushes can be produced on CHSSs by SI-ATRP technique from this simple, one-step initiator immobilization.

CONCLUSIONS

This report demonstrates that it is possible to use a free radical reaction to efficiently modify the CHSSs surface. The SI-ATRP technique was used to graft PSt and PMMA chains on

CHSSs both in the presence and in the absence of free initiator. It is noteworthy, that in addition to the single step initiator grafting, that the CHSSs did not require any acid treatment prior to the functionalization. SEM and TEM confirmed that the morphology of the CHSSs was unaltered during initiator fixation and SI-ATRP, and the CHSSs were homogeneously and evenly covered with a layer of PSt or PMMA (13–47-nm thick). It is expected that these grafted CHSSs could be efficient fillers for the fabrication of reinforced polymer as the presence of grafted polymer should increase the polymer-CHSSs interaction, thus ensuring an excellent load transfer.

ACKNOWLEDGMENTS

ME and SMG would like to acknowledge the Tulane Program for Bridge Research Support and the Gulf of Mexico Research Initiative (2012-II-798) for support, VTJ acknowledges the PKSFI grant program through the University of New Orleans and NSP acknowledges the NSF (CBET-1034175).

REFERENCES AND NOTES

- 1 N. G. Shang, T. Staedler, X. Jiang, *Appl. Phys. Lett.* **2006**, *89*, 103112-1–103112-3.
- 2 C. Wu, J. Chang, *Mater. Lett.* **2007**, *61*, 2502–2505.
- 3 Y. Y. Song, Y. Li, X. H. Xia, *Electrochem. Commun.* **2007**, *9*, 201–205.
- 4 J. Qiu, Y. Li, Y. Wang, C. Liang, T. Wang, D. Wang, *Carbon* **2003**, *41*, 767–772.
- 5 D. Pradhan, M. Sharon, *Mater. Sci. Eng. B* **2002**, *96*, 24–28.
- 6 S. Zhao, C. Y. Wang, M. M. Chen, J. H. Sun, *Carbon* **2009**, *47*, 331–347.
- 7 S. Kim, E. Shibata, R. Sergiienko, T. Nakamura, *Carbon* **2008**, *46*, 1523–1529.
- 8 Y. Ma, Z. Hu, K. Huo, Y. Lu, Y. Hu, Y. Liu, J. Hu, Y. Chen, *Carbon* **2005**, *43*, 1667–1672.
- 9 J. Y. Miao, D. W. Hwang, K. V. Narasimhulu, P. I. Lin, Y. T. Chen, S. H. Lin, L.P. Hwang, *Carbon* **2004**, *42*, 813–822.
- 10 M. Washiyama, M. Sakai, M. Inagaki, *Carbon* **1988**, *26*, 303–307.
- 11 Q. Wang, H. Li, L. Chen, X. Huang, *Carbon* **2001**, *39*, 2211–2214.
- 12 A. Deshmukh, S. D. Mhlanga, N. J. Coville, *Mater. Sci. Eng. R.* **2010**, *70*, 1–28.
- 13 M. M. Titirici, M. Antonietti, *Chem. Soc. Rev.* **2010**, *39*, 103–116.
- 14 Y. Z. Jin, C. Gao, W. K. Hsu, Y. Zhu, A. Huczko, M. Bystrzejewski, M. Roe, C. Y. Lee, S. Acquah, H. Kroto, D. R. M. Walton, *Carbon* **2005**, *43*, 1944–1953.
- 15 Z. C. Kang, Z. L. Wang, *Philos. Mag. B* **1996**, *73*, 905–929.
- 16 T. Liu, Q.; S. J. Jia, T. Kowalewski, K. Matyjaszewski, R. Casado-Portilla, J. Belmont, *Langmuir* **2003**, *19*, 6342–6345.
- 17 S. G. Vilt, N. Martin, C. McCabe, G. K. Jennings, *Tribol. Int.* **2011**, *44*, 180–186.
- 18 J. E. St. Dennis, K. Jin, V. T. John, N. S. Pesika, *ACS Appl. Mater. Interfaces* **2011**, *3*, 2215–2218.
- 19 X. Yang, J. Shi, S. Johnson, B. Swanson, *Langmuir* **1998**, *14*, 1505–1507.
- 20 O. Prucker, J. R uhe, *Langmuir* **1998**, *14*, 6893–6898.

- 21 P. K. Sudeep, Z. Page, T. Emrick, *Chem. Commun.* **2008**, *46*, 6126–6127.
- 22 S. Edmondson, V. L. Osborne, W. T. S. Huck, *Chem. Soc. Rev.* **2004**, *33*, 14–22.
- 23 Y. Tsujii, K. Ohno, S. Yamamoto, A. Goto, T. Fukuda, *Adv. Polym. Sci.* **2006**, *197*, 1–45.
- 24 R. Barbey, L. Lavanant, D. Paripovic, N. Schüwer, C. Sugnaux, S. Tugulu, H. A. Klok, *Chem. Rev.* **2009**, *109*, 5437–5527.
- 25 M. Ejaz, S. Yamamoto, K. Ohno, Y. Tsujii, T. Fukuda, *Macromolecules* **1998**, *31*, 5934–5936.
- 26 R. E. Behling, B. A. Williams, B. L. Staade, L. M. Wolf, E. W. Cochran, *Macromolecules* **2009**, *42*, 1867–1872.
- 27 Q. Wei, J. Ji, J. Shen, *Macromol. Rapid Commun.* **2008**, *29*, 645–650.
- 28 E. Marutani, S. Yamamoto, T. Ninjbadgar, Y. Tsujii, T. Fukuda, M. Takano, *Polymer* **2004**, *45*, 2231–2235.
- 29 J. M. Horton, Z. Bai, X. Jiang, D. Li, T. P. Lodge, B. Zhao, *Langmuir* **2011**, *27*, 2019–2027.
- 30 P. Jain, J. Dai, S. Grajales, S. Saha, G. L. Baker, M. L. Bruening, *Langmuir* **2007**, *23*, 11360–11365.
- 31 A. Carlmark, E. E. Malmström, *Biomacromolecules* **2003**, *4*, 1740–1745.
- 32 J. Pyun, K. Matyjaszewski, T. Kowalewski, D. Savin, G. Patterson, G. Kickelbick, N. Huesing, *J. Am. Chem. Soc.* **2001**, *123*, 9445–9446.
- 33 J. Pyun, T. Kowalewski, K. Matyjaszewski, *Macromol. Rapid Commun.* **2003**, *24*, 1043–1059.
- 34 Y. L. Liu, W. H. Chen, *Macromolecules* **2007**, *40*, 8881–8886.
- 35 Q. Yang, L. Wang, W. D. Xiang, J. F. Zhou, Q. H. Tan, *J. Polym. Sci. Part A: Polym. Chem.* **2007**, *45*, 3451–3459.
- 36 Q. Yang, L. Wang, J. Huo, J. Ding, W. Xiang, *J. Appl. Polym. Sci.* **2010**, *117*, 824–827.
- 37 Z. Yao, N. Braid, G. A. Botton, A. Adronov, *J. Am. Chem. Soc.* **2003**, *125*, 16015–16024.
- 38 S. H. Lee, D. R. Dreyer, J. An, A. Velamakanni, R. D. Piner, S. Park, Y. Zhu, S. O. Kim, C. W. Bielawski, R. S. Ruoff, *Macromol. Rapid Commun.* **2010**, *31*, 281–288.
- 39 Y. Z. Jin, C. Gao, H. W. Kroto, T. Maekawa, *Macromol. Rapid Commun.* **2005**, *26*, 1133–1139.
- 40 S. Banerjee, T. Hemraj-Benny, S. S. Wong, *Adv. Mater.* **2005**, *17*, 17–29.
- 41 N. Tsubokawa, *Polym. J.* **2005**, *37*, 637–655.
- 42 K. Ohkita, N. Tsubokawa, E. Saitoh, M. Noda, N. Takashima, *Carbon* **1975**, *13*, 443–448.
- 43 K. Ohkita, N. Tsubokawa, E. Saitoh, *Carbon* **1978**, *16*, 41–45.
- 44 Y. Ying, R. K. Saini, F. Liang, A. K. Sadana, W. E. Billups, *Org. Lett.* **2003**, *5*, 1471–1473.
- 45 B. Fragneaud, K. Masenelli-Varlot, A. Gonzalez-Montiel, M. Terrones, J.-Y. Cavaillé, *Chem. Phys. Lett.* **2006**, *419*, 567–573.
- 46 B. Hazer, *Eur. Polym. J.* **1990**, *26*, 1167–1170.
- 47 Y. Sun, Y. Wu, L. Chen, Z. Fu, Y. Shi, *Polym. J.* **2009**, *41*, 954–960.
- 48 J. B. Donnet, *Carbon* **1968**, *6*, 161–176.
- 49 M. Holzinger, O. Vostrowsky, A. Hirsch, F. Hennrich, M. Kappes, R. Weiss, F. Jellen, *Angew. Chem. Int. Ed. Engl.* **2001**, *40*, 4002–4005.
- 50 K. Matyjaszewski, J. H. Xia, *Chem. Rev.* **2001**, *101*, 2921–29.
- 51 K. Ohno, K. -M. Koh, Y. Tsujii, T. Fukuda, *Macromolecules* **2002**, *35*, 8989–8993.
- 52 Carlmark, E. Malmstroem, *J. Am. Chem. Soc.* **2002**, *124*, 900–901.
- 53 T. von Werne, T. E. Patten, *J. Am. Chem. Soc.* **2001**, *123*, 7497–7505.
- 54 K. Matyjaszewski, T. E. Patten, J. H. Xia, *J. Am. Chem. Soc.* **1997**, *119*, 674–680.
- 55 D. Hwang, A. Nomura, J. Kim, J.-H. Kim, H. Cho, C. Lee, K. Ohno, Y. Tsujii, *J. Nanosci. Nanotechnol.* **2012**, *12*, 4137–4141.